

Air Force Institute of Technology

**AFIT Scholar**

---

Faculty Publications

---

12-2017

## Self-trapped Holes in $\beta$ -Ga<sub>2</sub>O<sub>3</sub> Crystals

Brant E. Kananen

Nancy C. Giles

*Air Force Institute of Technology*

Larry E. Halliburton

*West Virginia University*

G. K. Foundos

*Northrop Grumman Synoptics*

K. B. Chang

*Northrop Grumman Synoptics*

*See next page for additional authors*

Follow this and additional works at: <https://scholar.afit.edu/facpub>



Part of the [Atomic, Molecular and Optical Physics Commons](#), and the [Semiconductor and Optical Materials Commons](#)

---

### Recommended Citation

B.E. Kananen, N.C. Giles, L.E. Halliburton, G.K. Foundos, K.B. Chang, and K.T. Stevens, *J. Appl. Phys.* 122, 215703 (2017).

This Article is brought to you for free and open access by AFIT Scholar. It has been accepted for inclusion in Faculty Publications by an authorized administrator of AFIT Scholar. For more information, please contact [richard.mansfield@afit.edu](mailto:richard.mansfield@afit.edu).

---


**Authors**

Brant E. Kananen, Nancy C. Giles, Larry E. Halliburton, G. K. Foundos, K. B. Chang, and K. T. Stevens

# Self-trapped holes in $\beta$ -Ga<sub>2</sub>O<sub>3</sub> crystals

Cite as: J. Appl. Phys. **122**, 215703 (2017); <https://doi.org/10.1063/1.5007095>

Submitted: 29 September 2017 . Accepted: 14 November 2017 . Published Online: 05 December 2017

B. E. Kananen , N. C. Giles, L. E. Halliburton, G. K. Foundos, K. B. Chang, and K. T. Stevens



View Online



Export Citation



CrossMark

## ARTICLES YOU MAY BE INTERESTED IN

[Oxygen vacancies and donor impurities in  \$\beta\$ -Ga<sub>2</sub>O<sub>3</sub>](#)

Applied Physics Letters **97**, 142106 (2010); <https://doi.org/10.1063/1.3499306>

[Iron and intrinsic deep level states in Ga<sub>2</sub>O<sub>3</sub>](#)

Applied Physics Letters **112**, 042104 (2018); <https://doi.org/10.1063/1.5020134>

[On the feasibility of p-type Ga<sub>2</sub>O<sub>3</sub>](#)

Applied Physics Letters **112**, 032108 (2018); <https://doi.org/10.1063/1.5009423>

Meet the Next Generation  
of Quantum Analyzers

And Join the Launch  
Event on November 17th



Register now



Zurich  
Instruments



## Self-trapped holes in $\beta$ -Ga<sub>2</sub>O<sub>3</sub> crystals

B. E. Kananen,<sup>1</sup> N. C. Giles,<sup>1</sup> L. E. Halliburton,<sup>2,a)</sup> G. K. Foundos,<sup>3</sup> K. B. Chang,<sup>3</sup>  
 and K. T. Stevens<sup>3</sup>

<sup>1</sup>Department of Engineering Physics, Air Force Institute of Technology, Wright-Patterson Air Force Base, Ohio 45433, USA

<sup>2</sup>Department of Physics and Astronomy, West Virginia University, Morgantown, West Virginia 26505, USA

<sup>3</sup>Northrop Grumman Synoptics, 1201 Continental Blvd., Charlotte, North Carolina 28273, USA

(Received 29 September 2017; accepted 14 November 2017; published online 5 December 2017)

We have experimentally observed self-trapped holes (STHs) in a  $\beta$ -Ga<sub>2</sub>O<sub>3</sub> crystal using electron paramagnetic resonance (EPR). These STHs are an intrinsic defect in this wide-band-gap semiconductor and may serve as a significant deterrent to producing usable *p*-type material. In our study, an as-grown undoped *n*-type  $\beta$ -Ga<sub>2</sub>O<sub>3</sub> crystal was initially irradiated near room temperature with high-energy neutrons. This produced gallium vacancies (acceptors) and lowered the Fermi level. The STHs (i.e., small polarons) were then formed during a subsequent irradiation at 77 K with x rays. Warming the crystal above 90 K destroyed the STHs. This low thermal stability is a strong indicator that the STH is the correct assignment for these new defects. The  $S = 1/2$  EPR spectrum from the STHs is easily observed near 30 K. A holelike angular dependence of the *g* matrix (the principal values are 2.0026, 2.0072, and 2.0461) suggests that the defect's unpaired spin is localized on one oxygen ion in a nonbonding *p* orbital aligned near the *a* direction in the crystal. The EPR spectrum also has resolved hyperfine structure due to equal and nearly isotropic interactions with <sup>69,71</sup>Ga nuclei at two neighboring Ga sites. With the magnetic field along the *a* direction, the hyperfine parameters are 0.92 mT for the <sup>69</sup>Ga nuclei and 1.16 mT for the <sup>71</sup>Ga nuclei. *Published by AIP Publishing.* <https://doi.org/10.1063/1.5007095>

### I. INTRODUCTION

As gallium oxide ( $\beta$ -Ga<sub>2</sub>O<sub>3</sub>) is developed for use in various electronic and optical applications,<sup>1,2</sup> it is essential to identify and characterize the intrinsic and extrinsic point defects that may enhance or degrade device performance. Shallow donors, e.g., Si and Sn, have been extensively studied,<sup>3–7</sup> and more recently gallium vacancies and Mg acceptors have been investigated.<sup>8,9</sup> Thus far, however, there is little experimental electronic and structural information available about the self-trapped hole (STH), a widely recognized important intrinsic defect in  $\beta$ -Ga<sub>2</sub>O<sub>3</sub>. Motivation to study this defect is provided by computational results<sup>10,11</sup> which clearly show that these STHs can be formed in  $\beta$ -Ga<sub>2</sub>O<sub>3</sub>. Attention has been focused on the STHs because they serve as the precursor to the self-trapped excitons (STEs) that are responsible for the dominant luminescence observed near 370–380 nm in  $\beta$ -Ga<sub>2</sub>O<sub>3</sub> crystals.<sup>12–15</sup> As first described by Varley *et al.*,<sup>10</sup> a more fundamental consequence of STH formation in  $\beta$ -Ga<sub>2</sub>O<sub>3</sub> crystals is the effect they may have on *p*-type conductivity. Depending on the barrier for STH migration, the mobility of holes (i.e., free polarons) may be small in this material. Because of the importance of this intrinsic defect, we have initiated a study of STHs in  $\beta$ -Ga<sub>2</sub>O<sub>3</sub>.

The STHs will be thermally stable at sufficiently low temperature in  $\beta$ -Ga<sub>2</sub>O<sub>3</sub>, provided that other deep defects serve as the compensating stable electron traps. This allows the STHs to be studied as long-lived isolated paramagnetic centers.<sup>16–18</sup> Although STHs can be formed at room

temperature in  $\beta$ -Ga<sub>2</sub>O<sub>3</sub> (as seen in luminescence experiments), they will be short-lived because of recombination<sup>15</sup> if mobile electrons are available and also because of a small thermal activation energy for migration. In addition to low temperature, a low Fermi level is needed in  $\beta$ -Ga<sub>2</sub>O<sub>3</sub> to produce stable, long-lived STHs. The typical undoped  $\beta$ -Ga<sub>2</sub>O<sub>3</sub> crystals available at the present time are *n*-type and have a high Fermi level (near the conduction band). In these *n*-type crystals, electrons from neutral shallow donors or the conduction band will quickly annihilate any self-trapped holes formed during an irradiation or illumination, even at low temperature. Thus, our study of long-lived isolated STHs is dependent on having a sample with a sufficiently low Fermi level as well as having deep traps to separately stabilize electrons.

In this paper, electron paramagnetic resonance (EPR) is used to observe the STHs in a  $\beta$ -Ga<sub>2</sub>O<sub>3</sub> crystal. These defects are thermally stable below approximately 80–100 K. The STHs are produced during an irradiation at 77 K with x rays, after using an irradiation with fast neutrons to lower the Fermi level of the crystal. The angular dependence of the STH spectrum provides the principal values and principal-axis directions of the *g* matrix and supports a model in which the hole (i.e., the unpaired spin) is localized in a nonbonding *p* orbital at a threefold-coordinated oxygen ion. Resolved hyperfine structure is due to equal interactions with the <sup>69</sup>Ga and <sup>71</sup>Ga nuclei at two neighboring sixfold-coordinated Ga sites.

### II. EXPERIMENTAL DETAILS

The  $\beta$ -Ga<sub>2</sub>O<sub>3</sub> crystal used in our study was grown by the Czochralski method at Northrop Grumman Synoptics

<sup>a)</sup>Author to whom correspondence should be addressed: Larry.Halliburton@mail.wvu.edu

(Charlotte, NC). Although not intentionally doped, the crystal was *n* type because of Si ions present in the starting materials. The crystal also contained trace amounts of Fe ions. When substituting for  $\text{Ga}^{3+}$ , this impurity may be present in the crystal as  $\text{Fe}^{2+}$ ,  $\text{Fe}^{3+}$ , or  $\text{Fe}^{4+}$ . The structure of  $\beta\text{-Ga}_2\text{O}_3$  is monoclinic with space group  $C2/m$  ( $C_{2h}^3$ ). Lattice constants<sup>19,20</sup> at  $273^\circ\text{C}$  are  $a = 12.214 \text{ \AA}$ ,  $b = 3.0371 \text{ \AA}$ ,  $c = 5.7981 \text{ \AA}$ , and  $\beta = 103.83^\circ$ . This complex binary crystal has two inequivalent gallium sites and three inequivalent oxygen sites. The Ga(I) ions have four oxygen neighbors and the Ga(II) ions have six oxygen neighbors. The O(I) and O(II) ions have three gallium neighbors and the O(III) ions have four gallium neighbors. A ball-and-stick representation of the crystal is shown in Fig. 1.

A Bruker EMX spectrometer operating near 9.4 GHz was used to obtain the EPR spectra. The temperature was controlled with an Oxford helium-gas flow system, and the static magnetic field was measured with a Bruker teslameter. Sample dimensions were approximately  $3.0 \times 1.5 \times 5.0 \text{ mm}^3$ . The  $\beta\text{-Ga}_2\text{O}_3$  crystal was neutron-irradiated for 3 h in the central irradiation facility of the Ohio State University Research Reactor (Columbus, OH). The total flux was  $\sim 2.1 \times 10^{13} \text{ neutrons cm}^{-2} \text{ s}^{-1}$  and the thermal flux was  $\sim 1.3 \times 10^{13} \text{ neutrons cm}^{-2} \text{ s}^{-1}$ . This irradiation lowered the Fermi level in the crystal as gallium-vacancy acceptors<sup>8</sup> were formed by displacement events initiated by the high-energy neutrons. The STHs were then produced during an x-ray irradiation at 77 K. An OEG-76H x-ray tube from Varian (operating at 60 kV and 30 mA) was used with an irradiation time of 5 min. Following an irradiation, the sample was quickly transferred from the liquid nitrogen to the cold helium gas flowing through the microwave cavity. The x rays provided an efficient method to generate the STHs in the neutron-irradiated  $\beta\text{-Ga}_2\text{O}_3$  crystal. We also produced

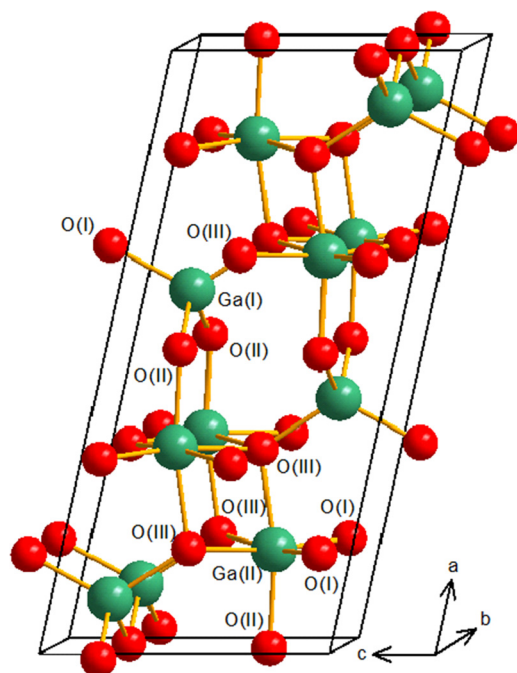


FIG. 1. Crystal structure of  $\beta\text{-Ga}_2\text{O}_3$ . Gallium ions are green and oxygen ions are red. The two inequivalent gallium sites are Ga(I) and Ga(II), and the three inequivalent oxygen sites are O(I), O(II), and O(III).

the STHs by illuminating the neutron-irradiated crystal with a small external Hg pen lamp while it was at 30 K in the microwave cavity.

### III. EPR RESULTS

Figure 2 shows the EPR spectrum from the STH in a  $\beta\text{-Ga}_2\text{O}_3$  crystal. This spectrum, taken at 30 K with the magnetic field along the *a* direction, was obtained immediately after an x-ray irradiation at 77 K of the previously neutron-irradiated crystal. A comparison with the recently reported  $\text{V}_{\text{Ga}}^{2-}$  and  $\text{Mg}_{\text{Ga}}^0$  spectra<sup>8,9</sup> shows that the hyperfine structure associated with the spectrum in Fig. 2 is distinctly different, thus demonstrating that this spectrum represents a new defect in  $\beta\text{-Ga}_2\text{O}_3$ . In a separate experiment, the STH spectrum in Fig. 2 was produced in an as-grown Mg-doped  $\beta\text{-Ga}_2\text{O}_3$  crystal during an illumination at 30 K with the Hg lamp. A difference curve of spectra taken at two different microwave powers after illumination revealed a weak STH signal underlying the larger  $\text{Mg}_{\text{Ga}}^0$  spectrum. This latter result from the Mg-doped crystal provides evidence that the new spectrum is a STH and removes the possibility that it represents a thus far unreported gallium-vacancy EPR spectrum from vacancies created during the neutron irradiation [e.g., a vacancy at a Ga(I) site instead of a Ga(II) site].<sup>8</sup> The STH

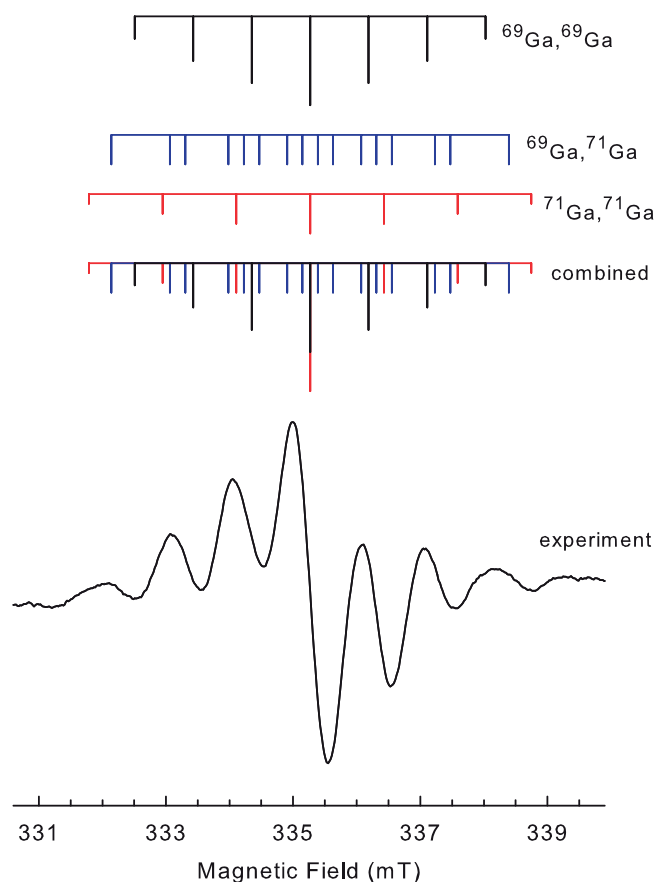


FIG. 2. EPR spectrum from the STH in  $\beta\text{-Ga}_2\text{O}_3$  taken at 30 K immediately after an x-ray irradiation at 77 K (the crystal had been previously neutron irradiated). The magnetic field is along the *a* direction and the microwave frequency is 9.3968 GHz. Stick diagrams above the spectrum refer to the hyperfine lines corresponding to different pairs of  $^{69}\text{Ga}$  and  $^{71}\text{Ga}$  nuclei at the two neighboring gallium sites.

spectrum was not observed in our previous study<sup>9</sup> of the neutral Mg acceptor in  $\beta$ -Ga<sub>2</sub>O<sub>3</sub> for several reasons. To produce the STH spectrum, the sample must be very quickly mounted and transferred into the cooled microwave cavity after an x-ray irradiation at 77 K (the Mg<sub>Ga</sub><sup>0</sup> acceptor does not become thermally unstable until near 250 K whereas the STH is thermally unstable above 80–100 K). Even more important, because of nearly identical  $g$  values and smaller Ga hyperfine spacings, the STH spectrum is completely overlapped by the Mg<sub>Ga</sub><sup>0</sup> spectrum for all orientations of magnetic field.

The spectrum from the STHs is symmetrical and consists of seven resolved hyperfine lines (the intensities progressively decrease on both sides of the middle line). Equivalent interactions with the <sup>69</sup>Ga and <sup>71</sup>Ga nuclei at two neighboring Ga sites are responsible for this hyperfine pattern. Both isotopes have an  $I=3/2$  nuclear spin, but their nuclear magnetic moments are different. The <sup>69</sup>Ga nuclei are 60.1% abundant with  $^{69}\mu = +2.0166\beta_n$  and the <sup>71</sup>Ga nuclei are 39.9% abundant with  $^{71}\mu = +2.5623\beta_n$ . Here,  $\beta_n$  represents the nuclear magneton. As reported earlier for the doubly ionized gallium vacancy<sup>8</sup> in  $\beta$ -Ga<sub>2</sub>O<sub>3</sub>, there are three combinations of the two Ga isotopes that contribute to the observed hyperfine pattern. These are (i) two <sup>69</sup>Ga nuclei, (ii) one <sup>69</sup>Ga nucleus and one <sup>71</sup>Ga nucleus, and (iii) two <sup>71</sup>Ga nuclei. The relative amounts of each combination are 36.1%, 48.0%, and 15.9%, respectively. A stick diagram for each combination is included above the experimental spectrum in Fig. 2. A “combined” stick diagram is also included, to allow easy comparison to the experimental spectrum. In these stick diagrams, the lengths of the vertical lines reflect the relative abundances of each pair of Ga nuclei. There are 29 individual lines contributing to the spectrum. However, because of the large linewidths and their overlapping nature, only the “envelopes” of seven sets of these lines are resolved.

The value of the magnetic field corresponding to the center of the STH spectrum varied noticeably for different directions of the field, indicating a nonisotropic  $g$  matrix. In contrast, the hyperfine splittings within the spectrum changed very little during rotations of the magnetic field. This suggests that the STHs can be described with nearly isotropic hyperfine matrices. Values for the hyperfine parameters are obtained from the experimental spectra. In Fig. 2, the lowest and highest lines in the <sup>69</sup>Ga-<sup>71</sup>Ga stick diagram are the dominant contributors to the lowest and highest lines in the experimental spectrum, located near 332.4 and 338.5 mT. The outer lines in the <sup>71</sup>Ga-<sup>71</sup>Ga stick diagram are more widely separated, but their intensities are a factor of three less than the outer lines in the <sup>69</sup>Ga-<sup>71</sup>Ga stick diagram, and thus they do not make the primary contribution to the outer experimental lines in Fig. 2. These lowest and highest lines in the experimental spectrum are separated by 6.21 mT. When the different magnetic moments of the nuclei are taken into account, this separation in magnetic field gives values of 0.92 and 1.16 mT for the <sup>69</sup>Ga and <sup>71</sup>Ga hyperfine parameters, respectively (for the magnetic field along the  $a$  direction). Using these hyperfine values for the two Ga sites and a linewidth of 0.50 mT, the SimFonia program from Bruker produced a simulated spectrum with lines occurring at the

TABLE I. Spin-Hamiltonian parameters for the STH in  $\beta$ -Ga<sub>2</sub>O<sub>3</sub>. Each STH interacts equally with Ga ions at two neighboring sites (<sup>69</sup>Ga and <sup>71</sup>Ga values are given for one of these two equivalent sites).

Direction of magnetic field	$g$ value	Hyperfine parameters (mT)	
		<sup>69</sup> Ga	<sup>71</sup> Ga
$a$ crystal axis	2.0026	0.92	1.16
$b$ crystal axis	2.0072	0.93	1.18
$c$ crystal axis	2.0461	0.90	1.14

same positions (i.e., with the same spacings) as in the experimental spectrum. Hyperfine parameters for the  $b$  and  $c$  directions were also obtained from the experimental spectra. These hyperfine results are listed in Table I.

Figure 3 shows the angular dependence resulting from the  $g$  matrix of the STH in  $\beta$ -Ga<sub>2</sub>O<sub>3</sub>. These data points, representing the middle of the hyperfine patterns, were taken every 10° during the rotation of the direction of the magnetic field from  $a$  to  $b$ ,  $b$  to  $c$ , and  $c$  to  $a^*$  to  $-c$ . Because  $a$  and  $c$  are 103.83° apart in this monoclinic structure, we introduce the  $a^*$  direction that is 90° from both  $b$  and  $c$ . Turning points in Fig. 3 occur at the  $a$  and  $c$  directions. These turning points place the principal axes of the  $g$  matrix approximately along the  $a$ ,  $b$ , and  $c$  directions in the crystal. A site splitting due to crystallographically equivalent, but magnetically inequivalent, orientations of the STH was not resolved in the angular dependence data, in agreement with  $a$ ,  $b$ , and  $c$  being the principal-axis directions. The corresponding principal values for the  $g$  matrix are listed in Table I. These principal values and the electron-Zeeman spin Hamiltonian ( $H = \beta\mathbf{S}\cdot\mathbf{g}\cdot\mathbf{B}$ ) were used to generate the solid curves in Fig. 3.

#### IV. MODEL OF THE SELF-TRAPPED HOLE

The present study describes a trapped-hole defect in  $\beta$ -Ga<sub>2</sub>O<sub>3</sub> that is very much like the previously reported doubly

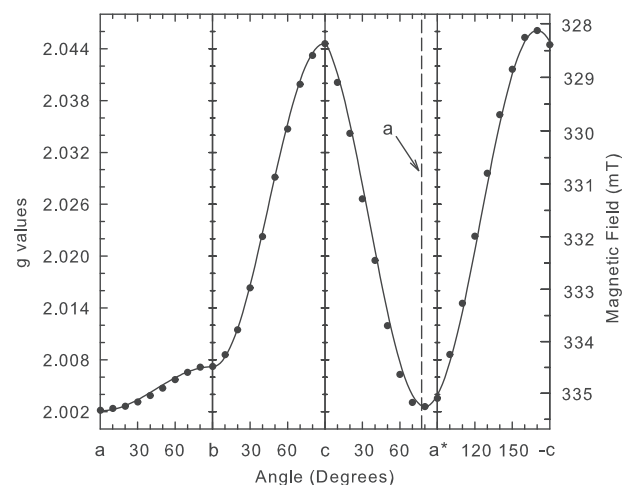


FIG. 3. Angular dependence associated with the  $g$  matrix of the STH. The shifts in the middle position of the STH spectrum are shown for rotations in three planes. Discrete points are experimental and the solid curves are computer-generated using the  $g$  values in Table I. Magnetic field values along the right vertical axis correspond to a microwave frequency of 9.3968 GHz.

ionized gallium vacancy<sup>8</sup> and neutral Mg acceptor.<sup>9</sup> In all three cases, the hole is localized in a  $p_z$  orbital on one oxygen ion, i.e., the primary feature of each defect is an O<sup>-</sup> ion with its  $2p^5$  configuration ( $2p_x^2 2p_y^2 2p_z$ ). The positive  $g$  shifts for these defects are similar (they all have  $\Delta g < 0.05$ ) and are caused by the spin-orbit mixing of the crystal-field-split energy levels of the  $^2P$  state ( $L = 1$ ,  $S = 1/2$ ). A first-order analysis<sup>8,21</sup> predicts that one of the three principal values of the  $g$  matrix will be very near the free-spin value of 2.0023, and the corresponding principal-axis direction will be aligned along the  $p$  orbital containing the unpaired spin. In Table I, the value of 2.0026 for  $g_a$  is close to 2.0023. This indicates that the  $p_z$  orbital containing the unpaired electron spin is oriented nearly along the  $a$  direction in the crystal.

Our model for the STH in  $\beta$ -Ga<sub>2</sub>O<sub>3</sub> is shown in Fig. 4. The hole is located at an O(I) ion, in a nonbonding  $p$  orbital aligned along the  $a$  direction. Of the three distinct oxygen sites in the crystal, only the O(I) site for the hole is consistent with all observations. A fourfold coordinated O(III) site is an unlikely possibility because the four positive Ga neighbors make it less favorable energy-wise for self-trapping a hole when compared to the O(I) and O(II) sites with just three positive Ga neighbors. Of these threefold-coordinated sites, the O(II) site is eliminated from consideration because its nonbonding  $p$  orbital is along the  $c$  direction in the crystal, in conflict with our  $g$ -matrix analysis that places the nonbonding  $p$  orbital of the STH approximately along the  $a$  direction. As shown in Fig. 4, the nonbonding oxygen orbital at the O(I) ion is oriented approximately perpendicular to the plane defined by the three neighboring Ga ions, two Ga(II) and one Ga(I). This allows the hole (i.e., the unpaired spin) to avoid its positive Ga neighbors as much as possible. As expected, the model for the STH in Fig. 4 is similar to the previously established model for the neutral acceptor ( $\text{Mg}_{\text{Ga}}^0$ ) in  $\beta$ -Ga<sub>2</sub>O<sub>3</sub> crystals,<sup>9</sup> with the difference being that the acceptor has one of the two Ga(II) ions replaced by the Mg ion. Our model for the STH, based on experimental considerations, is consistent with the earlier computational results of Varley *et al.*<sup>10</sup>

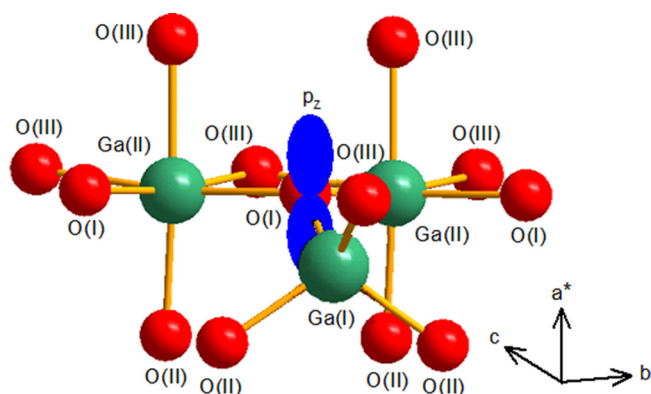


FIG. 4. Model of the STH in  $\beta$ -Ga<sub>2</sub>O<sub>3</sub>. The unpaired spin (the hole) is localized in a  $p_z$  orbital on a threefold oxygen ion O(I). The two adjacent Ga(II) ions are responsible for the resolved <sup>69</sup>Ga and <sup>71</sup>Ga hyperfine interactions observed in the EPR spectra. In order to self-trap the hole, the Ga(I) ion relaxes away from the O(I) ion.

Lattice relaxation is a primary requirement for a hole to be self-trapped. Small shifts in the positions of the neighboring ions provide the shallow potential well that localizes the hole on one oxygen ion. The most likely scenario for this relaxation has the Ga(I) ion in Fig. 4 moving away from the O(I) ion (with the hole) and toward the plane containing its remaining three neighboring oxygen ions. This displacement allows a more planar GaO<sub>3</sub> unit to form, consisting of the Ga(I) ion, the two O(II) ions, and the one O(III) ion, and increases the self-trapping energy of the STH. At the same time, the O(I) ion moves, to a lesser degree, toward the shifted Ga(I) ion and slightly away from the two neighboring Ga(II) ions. Our observation of equal hyperfine interactions with Ga nuclei at two equivalent Ga sites is consistent with this proposed lattice relaxation. In Fig. 4, the nuclei at the two equivalent Ga(II) sites are responsible for these resolved hyperfine interactions, while nuclei at the relaxed Ga(I) site are farther from the trapped hole and have a weaker, and experimentally unresolved, hyperfine interaction. Although detailed information is not provided, Varley *et al.*<sup>10</sup> show a relaxed configuration of the STH in  $\beta$ -Ga<sub>2</sub>O<sub>3</sub> that is similar to our suggested lattice distortion [see Fig. 1(b) in Ref. 10].

## V. THERMAL STABILITY

The thermal stability of the STH was determined by monitoring the intensity of its EPR spectrum as the crystal was progressively warmed to higher temperatures. An initial irradiation at 77 K with x rays produced the STHs and decreased the intensity of the spectrum from the doubly ionized gallium vacancies ( $V_{\text{Ga}}^{2-}$ ). The gallium vacancies were present in the crystal because of the earlier neutron irradiation.<sup>8</sup> After recording the EPR spectra from both defects at 30 K, the crystal was warmed to 90 K and held there for approximately 60 s, before returning to 30 K and taking the spectra again. Next, the crystal was warmed to 110 K, held for 60 s, and then returned to 30 K to record the spectra. This process was repeated at 130 and 150 K. Normalized changes in the intensities of the STH and  $V_{\text{Ga}}^{2-}$  acceptor spectra during these sequential heating steps are shown in Fig. 5. The vertical dashed line (at 77 K) in Fig. 5 for the  $V_{\text{Ga}}^{2-}$  spectrum represents the decrease in the concentration of the  $V_{\text{Ga}}^{2-}$  acceptors during the initial x-ray irradiation at 77 K.

The thermal anneal results shown in Fig. 5 are explained as follows. During the initial x-ray irradiation at 77 K, holes are trapped in the form of STHs. At the same time, electrons are trapped at  $V_{\text{Ga}}^{2-}$  acceptors, where they form triply ionized gallium vacancies ( $V_{\text{Ga}}^{3-}$ ). An EPR signal from singly ionized gallium vacancies ( $V_{\text{Ga}}^-$ ) was not observed after the irradiation.<sup>8</sup> The conversion of  $V_{\text{Ga}}^{2-}$  acceptors to nonparamagnetic  $V_{\text{Ga}}^{3-}$  acceptors explains the initial decrease in the concentration of  $V_{\text{Ga}}^{2-}$  acceptors (represented by the vertical dashed line in Fig. 5). Then, between 80 and 110 K, the STHs become thermally unstable and the holes migrate to  $V_{\text{Ga}}^{3-}$  acceptors where they form  $V_{\text{Ga}}^{2-}$  acceptors. This accounts for the observed increase in the  $V_{\text{Ga}}^{2-}$  spectrum as the STHs decay. The intensity of the Fe<sup>3+</sup> EPR spectrum in our crystal decreased by about a factor of two during the x-ray irradiation

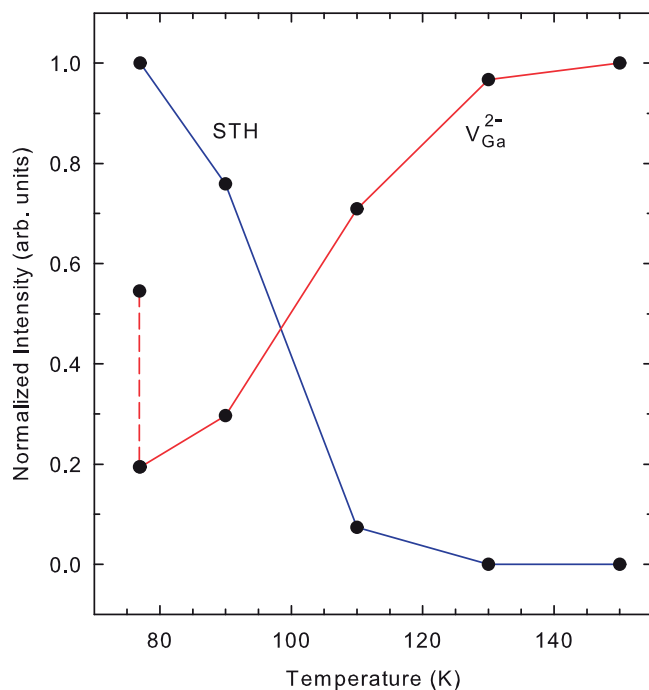


FIG. 5. Thermal stability of the STH in  $\beta$ - $\text{Ga}_2\text{O}_3$ . After the neutron irradiation and a subsequent x-ray irradiation at 77 K, the crystal was warmed in steps, with the EPR spectra of the STH (blue curve) and the doubly ionized gallium vacancy (red curve) monitored at 30 K after each step. The vertical dashed line represents the initial decrease in the gallium-vacancy spectrum. Both curves are normalized at their maximum intensities.

at 77 K, as the  $\text{Fe}^{3+}$  ions trap electrons and become  $\text{Fe}^{2+}$  ions. In  $\beta$ - $\text{Ga}_2\text{O}_3$ , the  $\text{Fe}^{2+}$  ions are not seen with EPR. A partial, but not complete, recovery of the intensity of the  $\text{Fe}^{3+}$  spectrum also occurs between 80 and 110 K, as some of the migrating holes from the STHs encounter  $\text{Fe}^{2+}$  ions. In Fig. 5, the intensity of the  $V_{\text{Ga}}^{2-}$  spectrum at 130 K is greater than its initial value before the x-ray irradiation. This suggests that a portion of the trapped electrons formed during the irradiation at 77 K are thermally stable to temperatures above 130 K.

In Fig. 5, approximately 22% of the STHs have thermally decayed after the 90 K anneal step and 96% are gone after the 110 K step. An activation energy for the thermal decay of these STHs can be estimated by using the approximation  $E \approx 23kT_m$ , where  $T_m$  corresponds to the temperature where half of the STHs have disappeared.<sup>22–24</sup> From the data in Fig. 5,  $T_m$  is  $\sim 97$  K and the estimated activation energy is  $\sim 190$  meV. The STHs thermally decay in our crystal when they have sufficient thermal energy to migrate through the lattice (i.e., by hopping from oxygen to oxygen) until they encounter a trapped electron. These electrons were stably trapped in the crystal during the initial x-ray irradiation near 77 K and are not mobile at the temperatures where the STHs begin to migrate. The STHs in our investigation (where the Fermi level in the crystal is low) do not decay because an electron returns to an STH, but rather because the holes move to trapped electrons. Thus, the observed STH decay in the 80–110 K region in our crystal is an intrinsic property of the STHs and does not depend on the specific identities of the participating electron traps.

## VI. SUMMARY

Electron paramagnetic resonance (EPR) has been used to observe self-trapped holes (STHs) in a  $\beta$ - $\text{Ga}_2\text{O}_3$  crystal. These STHs are produced when a crystal with a low Fermi level is irradiated at 77 K with x rays. They become thermally unstable when the temperature of the irradiated crystal is raised above 90 K, suggesting an activation energy for migration of about 190 meV. The unpaired spin of the STH is localized in a nonbonding  $p$  orbital on one threefold-coordinated oxygen. An angular-dependence study shows that this  $p$  orbital is aligned approximately along the  $a$  direction in the crystal. Partially resolved isotropic hyperfine interactions with  $^{69}\text{Ga}$  and  $^{71}\text{Ga}$  nuclei located at two equivalent neighboring sixfold-coordinated Ga sites are seen in the EPR spectra.

## ACKNOWLEDGMENTS

The authors acknowledge the technical assistance of Gregory W. Smith at the Air Force Institute of Technology (AFIT). This work was partially supported by the GHz-THz Electronics portfolio of the Air Force Office of Scientific Research (AFOSR). The views expressed in this paper are those of the authors and do not necessarily reflect the official policy or position of the Air Force, the Department of Defense, or the United States Government.

- <sup>1</sup>S. I. Stepanov, V. I. Nikolaev, V. E. Bougrov, and A. E. Romanov, "Gallium oxide: Properties and applications—A review," *Rev. Adv. Mater. Sci.* **44**, 63 (2016).
- <sup>2</sup>M. Higashiwaki, A. Kuramata, H. Murakami, and Y. Kumagai, "State-of-the-art technologies of gallium oxide power devices," *J. Phys. D: Appl. Phys.* **50**, 333002 (2017).
- <sup>3</sup>E. G. Vıllora, K. Shimamura, Y. Yoshikawa, T. Ujiie, and K. Aoki, "Electrical conductivity and carrier concentration control in  $\beta$ - $\text{Ga}_2\text{O}_3$  by Si doping," *Appl. Phys. Lett.* **92**, 202120 (2008).
- <sup>4</sup>J. B. Varley, J. R. Weber, A. Janotti, and C. G. Van de Walle, "Oxygen vacancies and donor impurities in  $\beta$ - $\text{Ga}_2\text{O}_3$ ," *Appl. Phys. Lett.* **97**, 142106 (2010).
- <sup>5</sup>K. Irmscher, Z. Galazka, M. Pietsch, R. Uecker, and R. Fornari, "Electrical properties of  $\beta$ - $\text{Ga}_2\text{O}_3$  single crystals grown by the Czochralski method," *J. Appl. Phys.* **110**, 063720 (2011).
- <sup>6</sup>D. Gogova, M. Schmidbauer, and A. Kwasniewski, "Homo- and heteroepitaxial growth of Sn-doped  $\beta$ - $\text{Ga}_2\text{O}_3$  layers by MOVPE," *CrystEngComm* **17**, 6744 (2015).
- <sup>7</sup>N. T. Son, K. Goto, K. Nomura, Q. T. Thieu, R. Togashi, H. Murakami, Y. Kumagai, A. Kuramata, M. Higashiwaki, A. Koukitu, S. Yamakoshi, B. Monemar, and E. Janzen, "Electronic properties of the residual donor in unintentionally doped  $\beta$ - $\text{Ga}_2\text{O}_3$ ," *J. Appl. Phys.* **120**, 235703 (2016).
- <sup>8</sup>B. E. Kananen, L. E. Halliburton, K. T. Stevens, G. K. Foundos, and N. C. Giles, "Gallium vacancies in  $\beta$ - $\text{Ga}_2\text{O}_3$  crystals," *Appl. Phys. Lett.* **110**, 202104 (2017).
- <sup>9</sup>B. E. Kananen, L. E. Halliburton, E. M. Scherrer, K. T. Stevens, G. K. Foundos, K. B. Chang, and N. C. Giles, "Electron paramagnetic resonance study of neutral Mg acceptors in  $\beta$ - $\text{Ga}_2\text{O}_3$  crystals," *Appl. Phys. Lett.* **111**, 072102 (2017).
- <sup>10</sup>J. B. Varley, A. Janotti, C. Franchini, and C. G. Van de Walle, "Role of self-trapping in luminescence and p-type conductivity of wide-band-gap oxides," *Phys. Rev. B* **85**, 081109(R) (2012).
- <sup>11</sup>P. Deak, Q. D. Ho, F. Seemann, B. Aradi, M. Lorke, and T. Frauenheim, "Choosing the correct hybrid for defect calculations: A case study on intrinsic carrier trapping in  $\beta$ - $\text{Ga}_2\text{O}_3$ ," *Phys. Rev. B* **95**, 075208 (2017).
- <sup>12</sup>E. G. Vıllora, K. Hatanaka, H. Odaka, T. Sugawara, T. Miura, H. Fukumura, and T. Fukuda, "Luminescence of undoped  $\beta$ - $\text{Ga}_2\text{O}_3$  single crystals excited by picosecond X-ray and sub-picosecond UV pulses," *Solid State Commun.* **127**, 385 (2003).



- <sup>13</sup>K. Shimamura, E. G. Villora, T. Ujiie, and K. Aoki, "Excitation and photoluminescence of pure and Si-doped  $\beta$ -Ga<sub>2</sub>O<sub>3</sub> single crystals," *Appl. Phys. Lett.* **92**, 201914 (2008).
- <sup>14</sup>M. Yamaga, T. Kishita, E. G. Villora, and K. Shimamura, "Relationship between persistent phosphorescence and electric conductivity in transparent conductive oxide  $\beta$  Ga<sub>2</sub>O<sub>3</sub>," *Opt. Mater. Express* **6**, 3135 (2016).
- <sup>15</sup>S. Yamaoka, Y. Furukawa, and M. Nakayama, "Initial process of photoluminescence dynamics of self-trapped excitons in a  $\beta$ -Ga<sub>2</sub>O<sub>3</sub> single crystal," *Phys. Rev. B* **95**, 094304 (2017).
- <sup>16</sup>A. M. Stoneham, J. Gavartin, A. L. Shluger, A. V. Kimmel, D. M. Ramo, H. M. Rønnow, G. Aeppli, and C. Renner, "Trapping, self-trapping and the polaron family," *J. Phys.: Condens. Matter* **19**, 255208 (2007).
- <sup>17</sup>O. F. Schirmer, "O<sup>-</sup> bound small polarons in oxide materials," *J. Phys.: Condens. Matter* **18**, R667 (2006).
- <sup>18</sup>S. Yang, A. T. Brant, and L. E. Halliburton, "Photoinduced self-trapped hole center in TiO<sub>2</sub> crystals," *Phys. Rev. B* **82**, 035209 (2010).
- <sup>19</sup>S. Geller, "Crystal structure of  $\beta$ -Ga<sub>2</sub>O<sub>3</sub>," *J. Chem. Phys.* **33**, 676 (1960).
- <sup>20</sup>J. Åhman, G. Svensson, and J. Albertsson, "A reinvestigation of  $\beta$ -gallium oxide," *Acta Crystallogr. C* **52**, 1336 (1996).
- <sup>21</sup>J. A. Weil and J. R. Bolton, *Electron Paramagnetic Resonance: Elementary Theory and Practical Applications*, 2nd ed. (John Wiley and Sons, Hoboken, New Jersey, 2007), Chap. 4, pp. 108–109.
- <sup>22</sup>J. T. Randall and M. H. F. Wilkins, "Phosphorescence and electron traps I. The study of trap distributions," *Proc. R. Soc. Lond. A* **184**, 366 (1945).
- <sup>23</sup>A. G. Milnes, *Deep Impurities in Semiconductors* (John Wiley and Sons, New York, 1973), Chap. 9, pp. 227–228.
- <sup>24</sup>S. V. Kondratenko, O. V. Vakulenko, Y. I. Mazur, V. G. Dorogan, E. Marega, Jr., M. Benamara, M. E. Ware, and G. J. Salamo, "Deep level centers and their role in photoconductivity transients of InGaAs/GaAs quantum dot chains," *J. Appl. Phys.* **116**, 193707 (2014).